Available online at www.sciencedirect.com
SCIENCE DIRECT®
Analytica Chimica Acta xxx (2006) xxx–xxx
ANALYTICA CHIMICA ACTA
www.elsevier.com/locate/aca

Capture and release of viruses using amino-functionalized silica particles

Zilin Chen [a], Fu-Chih Hsu [b], David Battigelli [b], Hsueh-Chia Chang [a,*]

[a] *Department of Chemical & Biomolecular Engineering, University of Notre Dame, Notre Dame, IN 46556, United States*
[b] *Scientific Methods Inc., 12441 Beckley Street, Granger, IN 46530, United States*

Received 27 January 2006; received in revised form 28 March 2006; accepted 28 March 2006

Abstract

A new virus capture/release strategy for the concentration of viral particles in water is reported. The method is an improvement upon traditional approaches that rely exclusively upon electrostatic attractions between a charged substrate and charged viral particles, which can only be reversed under extremely acidic or alkaline conditions to effect surface charge reversal and subsequent release of captured viruses. This method utilizes negatively charged silica beads functionalized with amino groups using defined length spacer molecules to yield particles with a surface density optimized for efficient virus capture. Following capture, viruses can be released using soluble proteins or amino acid-based alkaline eluents. Virus recoveries are a function of the composition of elution solution used. The zeta potentials of amino-functionalized silica particles were analyzed and used to optimize the density of functionalized groups and the charge behavior of the functionalized silica surfaces. Raman spectrometry was used for the characterization of functionalized silica beads. This method is expected to apply in the analysis of viruses.

Keywords: Functionalized silica; Virus concentration; Water sample; Zeta potential; Raman spectrometry

1. Introduction

More than 140 types of viruses are known to be excreted in feces by infected persons [1]. Several of these viruses are associated with waterborne transmission. The contamination of water with human enteric viruses continues to present a serious threat to the public health in many countries, including the United States. Enteric viruses can cause debilitating disease, and many outbreaks resulting from contaminated drinking water have been reported [2]. From 1971 to 1999, 9% of reported outbreaks of infectious disease associated with ground water contamination were attributed to viral agents. In 1982, 73 cases of hepatitis A virus (HAV) were documented to be the result of consuming contaminated water from a single spring in Meade County, Kentucky [3]. Norwalk virus and Norwalk-like viruses (noroviruses) are regarded as major causes of foodborne and waterborne viral gastroenteritis. Outbreaks of viral gastroenteritis have been associated with contamination of water supplies, raw foods and food products prepared by ill food handlers [4]. In 1995, an outbreak of norovirus gastroenteritis was linked to the failure of a septic tank system [5]. Results from several studies have indicated that conventionally treated drinking water may still contain human enteric viruses and cause outbreaks even when those waters have met water quality criteria based upon coliform bacteria densities and turbidity [6–9].

Because enteric viruses in general are infectious at relatively low concentrations, detection of virus samples in environmental waters typically requires the collection of large sample volumes (more than 1000 l). Adsorption-elution methods relying upon electrostatically charged microporous filters have been used extensively. Negatively charged materials, such as nitrocellulose (Millipore HA), fiberglas (Filterite) and cellulose (Whatman) are inexpensive but typically require extensive pre-conditioning of the water to facilitate binding interactions between the negatively charged surface material and negatively charged virus particles [10]. Pre-conditioning treatments may include acidification of the water sample or the addition of multivalent cationic salts (magnesium chloride or aluminum chloride) to serve as bridging molecules to facilitate virus capture. The addition of multivalent cations effects a charge reversal on the negatively charged viral particles, providing for electrostatic binding interactions on the filter surface. Alternatively, the counter-ion flux on the ion-selective membrane can produce a thick positively charged double layer near the membrane surface [11]. This

* Corresponding author. Tel.: +1 574 631 5697; fax: +1 574 631 8366.
E-mail address: hchang@nd.edu (H.-C. Chang).

0003-2670/$ – see front matter © 2006 Elsevier B.V. All rights reserved.
doi:10.1016/j.aca.2006.03.103

external double layer has a net charge higher than that of the membrane, thus effectively reversing the charge of the membrane to create a virus binding surface. The second mechanism can only occur if the pores are sufficiently small such that electro-osmotic flow and neutralizing convection are minimized, and only ion-selective electro-migration drives a cation flux into the membrane. As a result, negatively charged membrane filters generally must have small pore sizes (0.2–0.45 μm) to minimize internal flow, which severely restricts the volume of sample that can be filtered.

Electropositive filters have been described that can accommodate larger sample volumes due to their large porosity (10 μm) and extensive surface area [12,13]. However, the appreciable costs of these single-use products, coupled with erratic recoveries for some important viral agents preclude their routine use. Post-filtration processing also relies upon the use of relatively large volumes (~1000 ml) of highly alkaline, protein-rich eluent (beef extract/glycine) that may interfere with downstream enzyme-based assay procedures, such as the polymerase chain reaction (PCR™) due to the high concentration of interfering mammalian-derived DNA in the eluents. The large elution volumes also require secondary concentration to render the sample compatible with assay procedures that rely upon mammalian cell cultures (20–30 ml). More recently, alternative elution procedures relying upon defined eluents (e.g. amino acids) have been described for the recovery of non-culturable viruses from water, with encouraging reductions in assay interferences [4,14]. Li et al. reported a method using positively charged filter media for concentration of enteric viruses. The positively charged filtered media is composed of $NaCO_3$, $AlCl_3$ and silica gel [15]. Recently, hollow fiber ultrafilters have been used to detect enteric viruses in a variety of water samples and recoveries in excess of 50% have been reported [16]. However, these ultrafilters are relatively expensive, must be pretreated to block non-specific adsorption, and samples must be recirculated through filter cartridges under pressure at relatively slow flow rates (200–300 ml/min). These requirements make it impractical to filter large volumes of water in the field. Thus, there is an absence of a simple, rapid and economical method for the concentration of enteric viruses in water.

This work reports the development of a simple, efficient and inexpensive virus capture material based upon amino-functionalized silica beads that will efficiently recover viral agents in water. An array of amino-functionalized, electropositive silica materials was developed and applied to capture model bacterial viruses (coliphage MS-2 and bacteriophage PRD-1) from seeded water samples. The amino-functionalized silica prototypes included 3-aminopropyl-functionalized silica (APS), 3-(ethylenediamino)propyl-functionalized silica (EPS), 3-(diethylenetriamino)propyl-functionalized silica (DPS) and lupamin-coated silica (LS), with chemical structures presented in Fig. 1. Viruses captured on the prototype beads were released using eluent solutions containing soluble proteins or amino acids and surfactants. The zeta potentials of the amino-functionalized silica particles were analyzed and used to establish an index for monitoring the density of the functionalized groups and the charge behavior of the functionalized silica surfaces. Raman spectroscopy is a promising tool for characterizing the chemical information of solid phase surface. Surface-enhanced Raman scattering (SERS) was demonstrated a good way for low-level detection of viral pathogens [17]. Raman spectrometry was used for characterizing the functionalized silica surfaces prior to and after virus capture. A discussion of the possible mechanisms of virus capture and release on the basis of double layer theory and intermolecular interactions is presented.

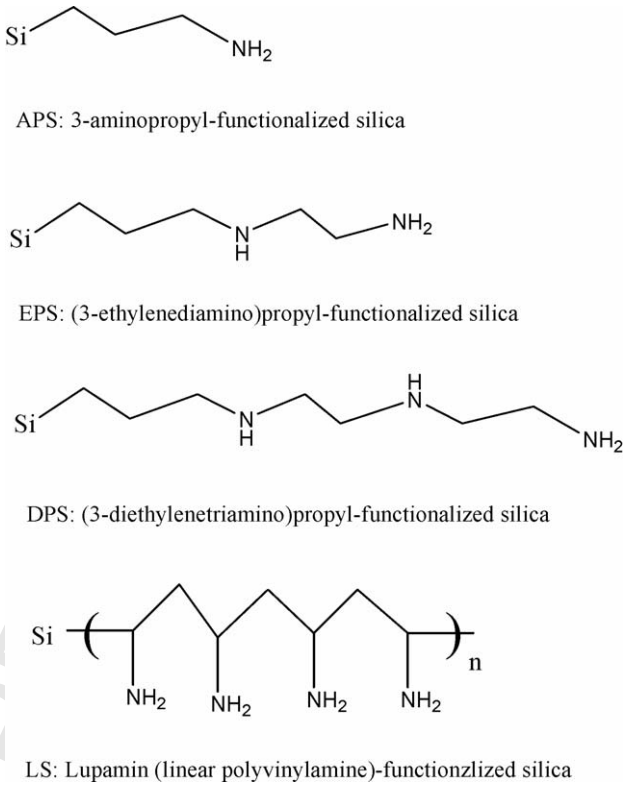

Fig. 1. Chemical structures of amino-functionalized silica.

2. Experimental

2.1. Preparation of amino-functionalized silica

An array of amino-functionalized silica bead products including 3-aminopropyl-functionalized silica, 3-(ethylenediamino)propyl-functionalized silica, 3-(diethylenetriamino)-propyl-functionalized silica and lupamin-coated silica was prepared according to the following reactions. Six grams of silica gel (70–270 mesh chromatography-grade, Sigma–Aldrich, Saint Louis, MO), was dried at 150 °C overnight, added to 150 ml of (3-aminopropyl)triethoxysilane in dry toluene. The slurry was refluxed for 20 h under continuous stirring. The APS amino-modified silica gels thus obtained were filtered, washed with toluene, acetone and methanol, and then dried at 105 °C for 4 h [18]. EPS was prepared as for APS, except for using [3-[(2-aminoethyl)amino]propyl]trimethoxysilane in place of (3-aminopropyl)triethoxysilane. DPS was prepared by adding 6 g of silica gel in 150 ml of 3% *N*-3-(trimethoxysilylpropyl)diethylenetriamine in 1 mM acetic acid

with continuous stirring for 3 h, filtering and washing with water and drying at 105 °C for 4 h [19]. Lupamin-coated silica (LS) was prepared by mixing 2 g of silica with 20 ml of 2 mg/ml polyvinylamine and stirring for 3 h. The resulting product was washed with water and dried for use.

2.2. Measurement of zeta potentials and Raman spectroscopy

Zeta potentials of functionalized silica particles were measured with a zeta Potential Analyzer (Brookhaven Instruments Corporation, Holtsville, NY). Particles were suspended in deionized water or phosphate buffers adjusted for pH. The Raman spectra of functionalized silica were measured with an inVia Raman Microscope (Renishaw, UK).

2.3. Preparation of bacteriophages MS-2 and PRD-1

Bacteriophages MS-2 (ATCC 15597-B1) and PRD-1 (BAA-769-B1) and *E. coli* Famp host bacteria (ATCC 700801) were purchased from the American Type Culture Collection (Gaithersburg, MD). Bacteriophages were plaque-purified and propagated to high titer using *E. coli* host cells according to the double agar layer infectivity method described by Adams [20], recovered in small volumes of phosphate-buffered saline, pooled and extracted using chloroform before aliquotting samples for use throughout the project. Virus stocks and host cells were archived in 20% glycerol (v/v) at −70 °C.

2.4. Determination of capture and elution efficiency

About 50 mg of silica particles with or without chemical functionalization were deposited into microcentrifuge tubes in duplicate and supplemented with 1 ml of bacteriophage MS-2 (approximately 100–200 plaque forming units (pfu) per unit volume). Silica/bacteriophage suspensions were vortexed every 30 s over a 5 min period. Tubes were then centrifuged for 2 min at 2000 × *g* at 10 °C, and supernatants were transferred to sterile polypropylene tubes. Pelleted beads were then supplemented with 1.0 ml of elution solution and vortexed every 30 s for a total 5 min, followed by centrifugation as before. The eluates were then transferred into fresh sterile tubes. The supernatants and eluates were then subjected to infectivity assay (double agar layer method) to identify the number of viable viruses captured and eluted from the functionalized silica beads. The typical elution solution was 1.5% beef extract, 0.25 M glycine and 0.01% Tween 80, unless otherwise stated.

2.5. Enumerative virus assay

Viruses were quantified according to the double agar layer method [20]. In brief, 0.1–0.5 ml of supernatant or sample eluate was added to 5 ml of molten top agar (0.9% wt./vol.) containing log-phase *E. coli* host from overnight cultures and poured into 100 mm plates containing nutrient bottom agar. After 16–24 h incubations at 37 °C, clear zones of lysis (viral 'plaques') were enumerated. Virus concentrations were determined as the mean sum of plaques across duplicate plates, corrected for dilution.

3. Results and discussion

3.1. Zeta potential, morphology and Raman spectroscopy of amino-functionalized silica

When particles are suspended in an electrolyte solution, a layer of counter ions exhibiting a charge opposite to those on the surface forms a charged double layer around the particle. The potential drop across the double layer is the zeta potential and its magnitude and sign reflects the density and charges of the surfaces. When functionalized groups are modified on the surface of the particle, the zeta potential can be altered because the functionalized groups change the surface charge and sometimes the thickness of the double layer due to the finite size of the functional group. We hence use the zeta potential as a measure of the density of the functionalized groups.

The zeta potential of bare silica gel in water (pH 7.0) was measured to be −27 to −35 mV, which indicates that silica exhibits a negatively charged surface in water, unsuitable for virus capture unless acidic conditions are imposed to effect charge reversal. The zeta potentials of amino-functionalized silica particles were measured as a function of pH condition, as shown in Fig. 2. Prior to chemical modification, bare silica shows a negative zeta potential above pH 3.0 due to the dissociation of protons from the silanol group. After chemical modification of the surface with amino groups, the amino groups can accept protons and become positively charged NH_3^+ species. As such, a positive zeta potential is detected under acidic conditions. Under alkaline conditions, the zeta potentials of LS, EPS and APS exhibit negative zeta potentials probably due to the dissociation of protons from the amino groups and the residual silanol (Si–OH) groups form $–NH_2$ and $Si–O^-$ species.

A key comparison is between the APS and DPS functionalized silica. As seen in Fig. 2, DPS can change the zeta potential more readily at alkaline conditions while APS is more effective at acidic conditions. Across the pH range of 4–8, the shift in zeta potential was relatively low (∼15 mV). This key differ-

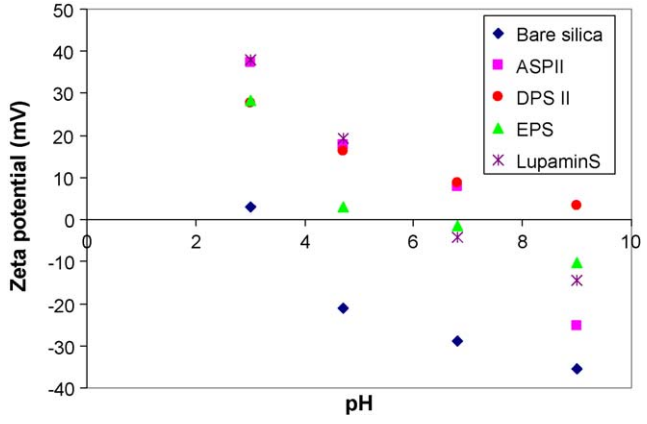

Fig. 2. pH effect on the zeta potentials of amino-functionalized silica. pH buffers were prepared with 10 mM phosphate buffer.

ence under conditions of extreme pH reflects the importance of the relative position of functional groups for the APS and DPS formulations shown in Fig. 1. APS amino groups are end groups that protonate to form $–NH_3^+$ whereas the DPS structure includes multiple $–NH_2^+$ functional groups within the silica matrix. These two sites have different titration features and different affinities for negatively charged viruses. It is known that the ionizable groups on the outer surface of the microorganism include carboxylic acids, organophosphates, amine and sometimes sulfate moieties [21]. Multiple NH_2^+ sites on the functionalized silica offer multiple hydrogen bonds for the functional groups on the surface of the virus particle, including carboxylic acids (–COOH). Because the hydrogen bond is a weaker intermolecular reaction, viruses captured by hydrogen bonding are more readily released.

The zeta potentials of bacteriophage MS-2 (pH 7.3 TSB) and bacteriophage PRD-1 (pH 7.6 TSB) were measured as −11.27 and −8.58 mV, respectively, reflecting the negative charges of these viruses aqueous solutions at neutral pH. The observed negative zeta potential is consistent with the isoelectric point (pI) of MS-2 previously determined as 3.9 [22]. Because the pI of MS2 falls below the pH of neutrality, the net charge on the outer surface of bacteriophage MS2 is negative. Based on these zeta potential measurements, it is clear that the amino-functionalized silica can possess an opposite charge from the virus and hence electrostatic attractions between the functional groups and the virus particles can be harnessed as a trapping mechanism.

The morphology of the silica particles was studied by scanning electron microscopy (SEM). As shown in Fig. 3, the shape of the silica particles is not uniform, and particle sizes ranged from approximately 50 to 100 μm with a distinct, non-porous surface. The Raman spectra of the bare silica and the amino-functionalized silica are presented in Fig. 4. According to the observed spectral shifts, functionalization of the bare silica resulted in a shift of peak absorbance from around 2000 to 2900 cm^{-1} for both the APS and DPS formulations. When the functionalized silica bead constructs were challenged with model viruses, the intensity of the observed spectral peaks

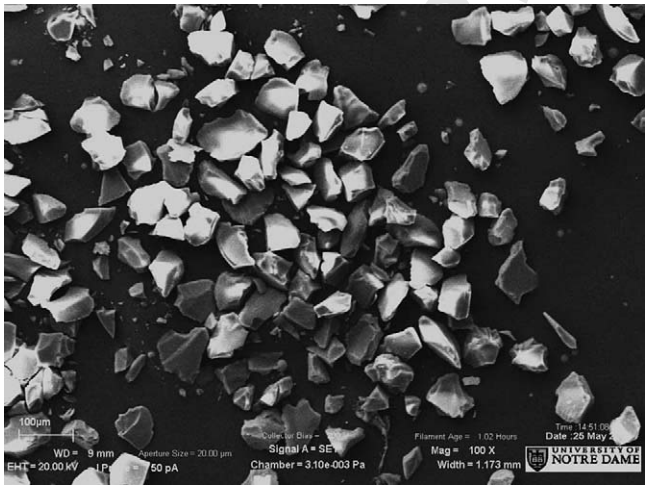

Fig. 3. Scanning electron microscopy images of silica particles.

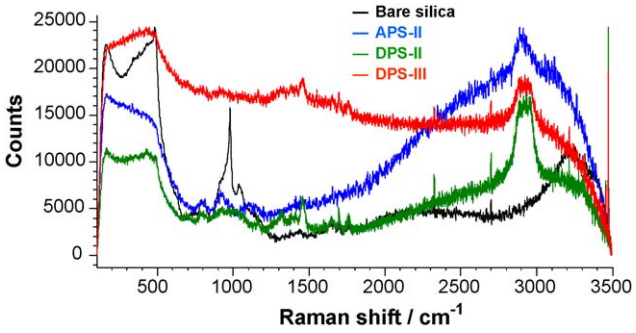

Fig. 4. Raman spectrum of amino-functionalized silica. Laser: 633 nm, grating: 1800 lines/mm, exposure time: 10 s and accumulations: 10 times.

Table 1
Zeta potential of functionalized silica particles following virus capture

Type of particle	Before	After capture (MS2)	After capture (PRD1)
Bare silica	−35.55	−36.77	−28.97
APS	9.18	−26.34	−5.4
DPS	22.32	−12.88	−0.5

Zeta potential of viruses in TSB; MS2: −11.7 mV, PRD1: −8.58 mV.

decreased, indicating an interaction between the functionalized amino groups and the coliphage particles.

3.2. Capture and release of virus using amino-functionalized silica

Table 1 shows the change in zeta potential exhibited by silica particles before and after virus capture. Because the bare silica preparations exhibit a negative charge they were ineffective in binding the negatively charged virus particles; the negligible shifts in zeta potential following challenge either with coliphage MS-2 or PRD-1 were consistent with this observation, when bare silica was challenged with coliphage. However, the zeta potentials of the APS and DPS constructs changed appreciably from positive to negative values following virus capture with both model microorganisms. This observation was consistent with the high efficiency virus binding that was observed with the two model coliphages (95.5–99.8%, Table 2) based on the intermolecular electrostatic attraction and specific interactions, such as hydrogen bonding between the viruses and functionalized amino groups.

Tables 2 and 3 show the capture and release efficiencies of the amino-functionalized silica constructs, respectively. Several models of virus capture are presented in Fig. 5. As expected, the bare silica exhibited poor virus binding efficiency (∼13%) due to electrostatic repulsion between the negatively charged virus

Table 2
Capture efficiency of virus

Sample	Capture efficiency MS2	Capture efficiency PRD1
Bare silica	13.3 ± 15.1	9.0 ± 12.3
APS II	99.8 ± 0.5	95.5 ± 3.3
DPS II	98.0 ± 1.6	95.3 ± 3.0
Lupamin Si	99.5 ± 0.6	99.0 ± 0

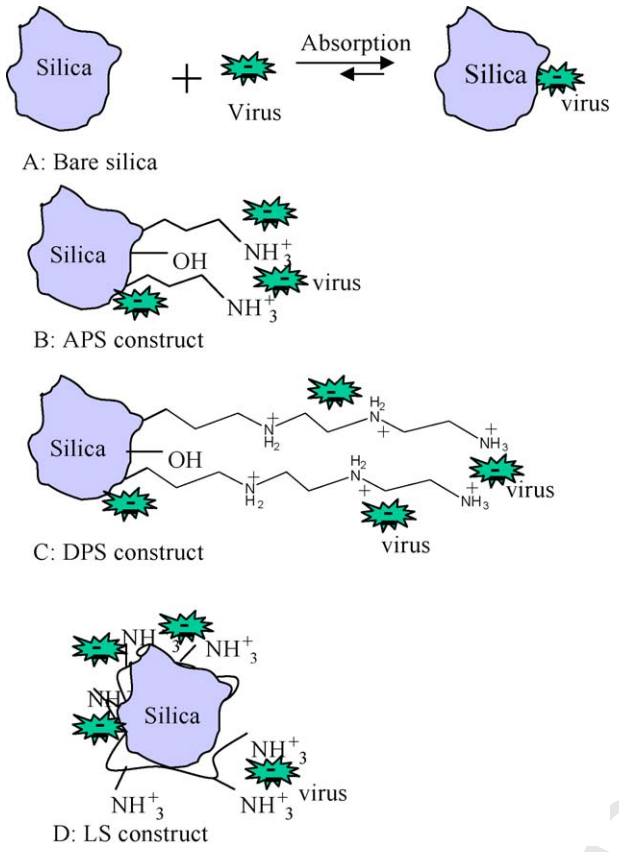

Fig. 5. Suggested models of virus capture on amino-functionalized silica.

surface and the negatively charged silanol groups following dissociation of a proton. The small level of virus capture observed (ca. 10%) may have been associated with physical adsorption of virus onto the silica surface as shown in Fig. 5A, or failure to wash away residual viruses from the aqueous supernatant. The high efficiency of virus capture observed for the APS, DPS and LS constructs (>98%) was attributed to the high density of positively charged amino groups, facilitating electrostatic attraction and other intermolecular interactions, such as hydrogen bonding.

Although the virus capture efficiencies of the three silica constructs were comparable, their capacities to release bound viruses were quite different (Table 3). Binding between coliphage MS-2 and the APS construct was essentially irreversible (4% of captured viruses could be released), however, interactions between this construct and coliphage PRD-1 could be readily reversed (~70% of bound viruses could be released). Conversely, coliphage MS-2 could be recovered readily from the DPS construct, whereas release of coliphage PRD-1 was relatively low (~32% of bound viruses could be recovered). Recoveries of model viruses from the lupamin construct were intermediate, ranging from essentially 0 (MS-2) to ~21% (PRD-1).

Table 3
Release efficiency of virus with 1.5% beef extract supplemented with 0.25 M glycine and 0.01% Tween 80

Sample	Release efficiency MS2	Release efficiency PRD1
Bare silica	3.9 ± 0.8	6.3 ± 3.7
APS II	4.0 ± 1.4	69.5 ± 3.5
DPS II	79.0 ± 10.7	31.9 ± 16.2
LS	0 ± 0	21.0 ± 1.4

These observations suggest that there are differences in the interactions between the model viruses and the different types of functionalized silica. A number of potential capture mechanisms are suggested in Fig. 5. As shown in Fig. 5D, lupamin is a long linear polyvinylamine, which is likely to manifest itself as an entangled conformation on the silica surface [23]. The thicknesses of the charged double layer in 1 and 100 mM KCl aqueous solutions are calculated to be 10 and 1 nm, respectively [24]. The length of a single carbon bond is known to be 0.154 nm [25]. The positively charged multiple amino groups on the surface of the silica and the virus capsid are hence likely to be surrounded by a double layer cloud. When protein-rich eluants are utilized to sever the connection between bound viruses and charged silica surfaces, this double layer 'screening' may eliminate the attractive force between suspended proteins and the silica-virus complex. As a result, virus binding cannot be readily reversed by substituting the virus binding site on the silica with a protein or surfactant molecule. The weaker PRD-1 charge density relative to MS-2 (−8.58 mV versus −11.27 mV) suggests that PRD-1 may be more readily substituted and released from each binding site. This is indeed true for the APS functionalized bead but not so for the DPS construct. The weaker hydrogen bonding between NH_2^+ groups on the DPS and the charged carboxylic acid groups on the virus surface would also suggest easier release.

The same reason would argue that DPS would exhibit the highest release efficiency for coliphage PRD-1. While a high release rate for this combination was observed (Table 3), the efficiency of release was approximately 50% of that observed for PRD-1 on the DPS construct. The observed reduction in release efficiency may have been associated with the fact that the DPS construct includes NH_2 sites that may exhibit comparable lengths with the –COOH and $–NH_2$ sites on the surface of the model coliphage (PRD-1) to the extent that multiple binding sites may be involved with each virus adsorption 'event'; viruses bound by multiple interactions may be more difficult to release than those bound by single intermolecular reactions. DPS exhibited the highest release efficiency for coliphage MS-2 (Table 3), probably due to the extended length of the DPS functional group and its rigid conformation, which may facilitate an interaction that allows the group to protrude inside the double layer and attract the substituting proteins and surfactants by intermolecular interactions, as shown in Fig. 5C.

3.3. Release of virus with different elution solutions

In order to adjust the zeta potential and improve the virus release efficiency, the traditional beef extract-based virus elution solution was modified to include surfactants and additional amino acids. Following the initial characterization of the virus binding properties of each silica matrix, we examined the effects

of these modified eluants upon the release efficiency of coliphage MS-2 using the APS construct. The following eluants were studied: 1.5% beef extract, 3.0% beef extract, defined amino acids including 0.5 M glycine and 0.5 M lysine, and surfactants, such as 0.1% cetyltrimethylammonium bromide (CTAB), 0.1% sodium dodecylsulfate (SDS) and 0.01% polysorbate (Tween 80). All combinations of eluant components studied exhibited poor elution efficiency (less than 4.5%) for coliphage MS-2 captured on the APS construct. As indicated in Figs. 1 and 5B, the aminopropyl group is relatively short and the captured MS-2 particle is screened by the double layer ion cloud such that the protein and surfactants cannot be attracted to the sites on the functional group to release the captured virus. Conversely, the APS construct has only a single $–NH_3^+$ group, which lacks multiple hydrogen bonding mechanism, resulting in low release efficiency.

The higher release efficiency of bacteriophage MS-2 exhibited by the DPS II construct was probably associated with the longer 3-(diethylenetriamino)propyl group that may protrude inside the double layer and offer multiple NH_2 sites for weaker hydrogen bonds. Among the elution solutions examined, 1.5% beef extract was the most essential component of the elution solution. When eluants were supplemented with 0.1% CTAB, elution efficiencies decreased. The addition of both 0.1% anionic surfactant (SDS) and 0.01–0.1% non-ionic surfactant (Tween 80) improved release efficiencies. Increasing the concentration of surfactant beyond 0.01% did not improve virus recoveries significantly. Use of defined component eluants (either lysine or glycine) did not result in efficient release of model viruses with the exception of 0.5 M lysine supplemented with 0.01% Tween 80.

The substitution of 0.25 M glycine (Gly) and 0.25 M threonine (Thr) for the primary eluent component (beef extract) resulted in a 42% virus release efficiency. This encouraging result suggests that it may be possible to remove beef extract from the eluent altogether, rendering the concentrates much more compatible with PCR-based assay techniques which otherwise may be inhibited substantially by the abundance of nucleic acids of calf origin arising from the beef extract-rich solutions. However, the highest release efficiency observed with these eluents (79%) was observed when 1.5% beef extract was supplemented with 0.25 M glycine and 0.01% Tween 80. Similar release characteristics were observed for bacteriophage PRD-1, where the elution efficiencies ranged from 30 to 43.5%.

3.4. pH effect on the capture efficiency

Since the pH of field samples varies considerably, it is important to determine the efficiency of virus capture using functionalized silica across a range of pH values. The results in Fig. 6 indicate that functionalized silica constructs DPS-VI and APS-II capture viruses very efficiently from pH 3 to 9. Overall, more than 98% of the seeded viruses were captured between pH 5 and pH 7. The highest capture efficiency was achieved at pH 7. Even at pH 9, both constructs exhibited capture efficiencies of ~98%. Under extremely acidic conditions (pH 3), the zeta potential is very high (Fig. 2) which suggests that the functionalized silica exhibits a high density of positive charge. However, as the isoelectric point (pI) of MS2 is 3.9 [22], when ambient pH falls below the pI, some of functional groups on the virus capsid exhibit positive charge, resulting in a decreased capture efficiency. Conversely, although viruses tend to be positively charged under extremely acidic conditions (pH < 3), the functionalized silica still exhibited a high capture efficiency, suggesting that the capture mechanism includes not only electrostatic attraction but also other multiple intermolecular interactions, such as hydrogen bondings. At pH 9 and higher, although the virus particles exhibit higher negative charges, the density of positive charge of functionalized silica is lower compared to acidic conditions. Hence, the capture efficiency is decreased at pH 9 compared to neutral conditions, such as pH 5–7. As the ionizable groups on the virus surface are carboxylic acids, organophosphates, amines and sometimes sulfate moieties [21], they can offer multiple point-specific interactions, such as hydrogen bonds to functionalize amino groups on the surface of silica.

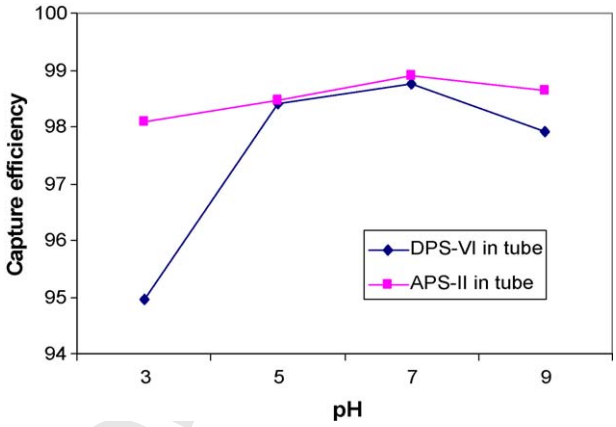

Fig. 6. pH effect on capture efficiency. Spiked concentrations of MS-2: 9.0×10^3 to 4.7×10^4 pfu/ml for DPS-VI and APS-II in tube, 740–887 pfu/ml for DPS-VI in a column and 2.9×10^5 to 1.1×10^6 pfu/ml.

3.5. Capacity of virus capture

It is important to understand the capture capacity under a wide range of virus concentrations for applying functionalized silica to field samples. To determine capture efficiencies across a range of virus concentrations, 10^3, 10^4 and 10^6 pfu of viral particles were seeded into 1 ml volumes of reagent water in microcentrifuge tubes. Viruses were captured by DPS-VI and released using 1.5% beef extract/0.25 M glycine/0.1% Tween 80 at pH 9.0. As indicated in Fig. 7, DPS-VI was capable of capturing 99.7% of the viruses seeded regardless of the spiking concentrations. These results demonstrate that the capture capacity of the functionalized silica material is more than sufficient to accommodate the range of virus concentrations that may be expected in natural waters. The good linear relationship between the concentrations of spike and recovery indicates that captured virus on the functionalized silica media can be dynamically released by a specific elution solution.

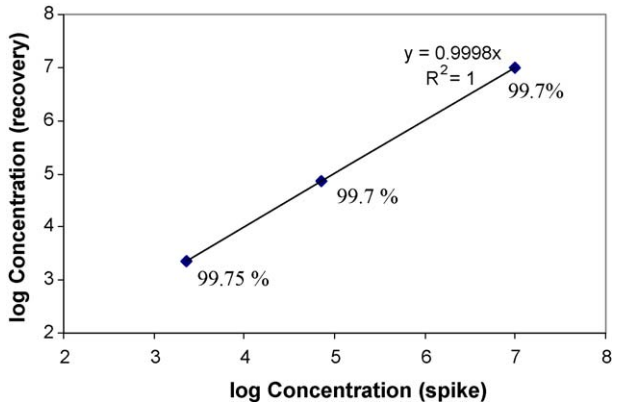

Fig. 7. Correlation between spiked and recovered concentrations of virus MS-2.

4. Conclusions

We have successfully developed an effective amino-functionalized silica material and applied it to water samples for capture and release of viruses. All the amino-functionalized silica materials including APS, DPS, EPS and LS can capture virus with efficiencies exceeding 95%. Because the 3-(diethylenetriamino)propyl group in the DPS construct relies upon hydrogen bonding with virus particles, these relatively weak interactions are more readily broken for efficient release of captured viruses. Hence, the 79% recoveries observed for bacteriophage MS-2 and 32% recoveries for PRD-1 captured on DPS using elution solutions containing 1.5% beef extract, 0.25 M glycine and 0.01% Tween 80 were not surprising. The results of the sequence of experiments on the effects of pH and virus concentration suggest that these functionalized silica materials are capable of capturing viruses quite efficiently across a wide range of virus concentrations and pH values. As viruses have long been very challenging to concentrate, these functionalized silica materials can be tailored towards a wide variety of virus filtering and concentration applications. The results from this study suggest that amino-functionalized silica particles may be applied to concentrate viruses in water samples with a wide range of pHs and virus densities. This method is expected to apply in the analysis of viruses. Further studies in concentrating viruses from large volumes of water will be carried out in the future.

Acknowledgements

We thank Prof. Hsien-Chang Chang at National Cheng-Kung University, Taiwan for his assistance with the Raman spectroscopy analyses. This work is supported through an SBIR grant from the U.S. Environmental Protection Agency (EPA-SBIR No: EP-D-05-037).

References

[1] C. Monceyron, B. Grinde, J. Virol. Methods 46 (1994) 157.
[2] R.I. George, in: Sherris (Ed.), Medical Microbiology, second ed., Elsevier, New York, 1990, pp. 537–546.
[3] G.H. Bergeisen, M.W. Hinds, J.W. Skaggs, Am. J. Public Health 75 (1985) 161.
[4] C.W. Hedberg, M.T. Osterholm, Clin. Microbiol. Rev. 6 (1993) 199.
[5] M. Bellar, A. Ellis, S.H. Lee, M.A. Drebot, JAMA 278 (1997) 563.
[6] T.R. Deetz, E.M. Smith, S.M. Goyal, C.P. Gerba, J.J. Vollet, L. Tsai, H.L. DuPont, B.H. Keswick, Water Res. 18 (1984) 567.
[7] C.P. Gerba, J.B. Rose, A. Gordon (Eds.), Drinking Water Microbiology, Spring-Verlag, New York, 1990.
[8] P. Payment, Can. J. Microbiol. 27 (1981) 417.
[9] K. Nygard, M. Torven, C. Anccke, K.B. Knauth, K.O. Hedlund, J. Giesecke, Y. Andersson, L. Svensson, Emerg. Infect. Dis. 9 (2003) 1548.
[10] J. Lukasik, T.M. Scott, D. Andryshak, S.R. Farrah, Appl. Environ. Microbiol. 66 (2000) 2914.
[11] Y. Ben, H.-C. Chang, J. Fluid Mech. 461 (2002) 229.
[12] M.D. Sobsey, B.L. Jones, Appl. Environ. Microbiol. 37 (1979) 588.
[13] M.D. Sobsey, J.S. Glass, Appl. Environ. Microbiol. 40 (1980) 201.
[14] L. Kittigul, P. Khamoun, D. Sujirarat, F. Utrarachkij, K. Chitpirom, N. Chaichantanakit, K. Vathanophas, Mem. Inst. Oswaldo Cruz. 96 (2001) 815.
[15] J.W. Li, X.W. Wang, Q.Y. Rui, N. Song, F.G. Zhang, Y.C. Ou, F.H. Chao, J. Virol. Methods 74 (1998) 99.
[16] H.A. Morales-Morales, G. Vidal, J. Olszewski, C.M. Rock, D. Dasgupta, K.H. Oshima, G.B. Smith, Appl. Environ. Microbiol. 69 (2003) 4098.
[17] J.D. Driskell, K.M. Kwarta, R.J. Lipert, M.D. Porter, J.D. Neill, J.F. Ridpath, Anal. Chem. 77 (2005) 6147.
[18] K. Fujimura, T. Ueda, T. Ando, Anal. Chem. 55 (1983) 446.
[19] X. Zhao, L. Hilliard, S. Mechery, Y. Wang, R. Bagwe, S. Jin, W. Tan, PNAS 101 (2004) 15028.
[20] M.H. Adams, Bacteriophages, Wiley-Interscience, New York, 1959.
[21] M.J. Desai, D.W. Armstrong, Microbiol. Mol. Biol. Rev. 67 (2003) 38.
[22] N.D. Zinder (Ed.), RNA Phages, Cold Spring Harbor Laboratory, New York, USA, 1975, pp. 7–8.
[23] I. Viogt, F. Simon, K. Estel, S. Spange, Langmuir 17 (2001) 3080.
[24] Brookhaven Instruments Corporation, Zeta Potential Analyzer Instruction Manual, p. 26.
[25] Jeremy K. Burdett, Chemical Bonding in Solids, Oxford University Press, New York, 1995, p. 152.